ARTICLES

Transition from strange nonchaotic to strange chaotic attractors

Ying-Cheng Lai

*Department of Physics and Astronomy, Department of Mathematics, Kansas Institute for Theoretical and Computational Science,
The University of Kansas, Lawrence, Kansas 66045*
(Received 15 September 1995)

We investigate the transition from strange nonchaotic to strange chaotic attractors in quasiperiodically driven dynamical systems. It is found that whether the asymptotic attractor of the system is strange nonchaotic or strange chaotic is determined by the relative weight of the contraction and expansion for infinitesimal vectors along a typical trajectory on the attractor. When the average contraction dominates the average expansion, the attractor is strange nonchaotic. Strange chaotic attractors arise when the average expansion dominates the average contraction. The transition from strange nonchaotic to strange chaotic attractors occurs when the average contraction and expansion are balanced. A characteristic signature of this route to chaos is that the Lyapunov exponent passes through zero *linearly*. We provide numerical confirmation using both a quasiperiodically driven map and a quasiperiodic flow.

PACS number(s): 05.45.+b

I. INTRODUCTION

Strange nonchaotic attractors occur in nonlinear dynamical systems [1–7]. Here the word *strange* refers to the complicated geometry of the attractor: a strange attractor contains an infinite number of points and it is not a smooth surface in the phase space. The word *chaotic* refers to the sensitive dependence on initial conditions: trajectories originating from nearby initial conditions on a chaotic attractor diverge exponentially in time. Strange nonchaotic attractors are therefore geometrically complicated; nonetheless, they exhibit no sensitive dependence on initial conditions. One example of strange nonchaotic attractors is the attractors in the one-dimensional logistic map $x_{n+1} = rx_n(1-x_n)$ at precisely the values of the parameter r where there is an accumulation of an infinite number of period doublings [8]. This set of r values for the occurrence of strange nonchaotic attractors in the logistic map is nevertheless a set of measure zero in the parameter space.

While strange nonchaotic attractors occur only at a set of measure zero parameter values for most dynamical systems with period-doubling bifurcations to chaos, the existence of these exotic attractors in dissipative dynamical systems driven by several *incommensurate* frequencies (quasiperiodically driven systems) was suggested in 1984 [1]. Subsequent works demonstrated that strange nonchaotic attractors occur commonly in quasiperiodically driven systems [2–7]. In particular, it was demonstrated that in two-frequency quasiperiodically driven systems, there exist parameter regions of finite area in the parameter space for which there are strange nonchaotic attractors [3,4]. In this sense, strange nonchaotic attractors are said to be "typical" in quasiperiodically driven systems. Experimental observation of a strange nonchaotic attrac-

tor was achieved by Ditto *et al.* [9]. One mechanism by which strange nonchaotic attractors are created was investigated by Heagy and Hammel [5], who discovered that, in quasiperiodically driven maps, the transition from a two-frequency quasiperiodic attractor to a strange nonchaotic attractor occurs when a period-doubled torus collides with its unstable parent torus [5]. Near the collision, the period-doubled torus becomes extremely wrinkled and develops into a fractal set at the collision, although the Lyapunov exponent remains negative throughout the collision process. More recently, methods to characterize strange nonchaotic attractors were proposed [6]. One method was based on analyzing the bifurcation structure of the systems resulting from periodic approximations of the quasiperiodic forcing. In another method, a phase sensitivity exponent that measures the sensitive dependence of trajectories on changes in the phase of the external forcing was proposed to characterize the strangeness of the attractors. It was shown that such an exponent can assume positive values even though the Lyapunov exponent is nonpositive [6]. The most important observation was that a trajectory on a strange nonchaotic attractor actually possesses positive Lyapunov exponents in finite-time intervals, although asymptotically, the exponent is negative. Other works on strange nonchaotic attractors include a renormalization analysis for the birth of these attractors [10] and their correlation and spectrum properties [7].

In this paper we investigate how a strange nonchaotic attractor, after its birth, may change into a different type of attractor as a system parameter is varied further. Specifically, we are interested in how the transition from strange nonchaotic to strange chaotic attractor occurs in quasiperiodically driven systems. Our investigation is motivated by the observation that a chaotic attractor

differs from a strange nonchaotic attractor *only* in the dynamical properties as characterized by the Lyapunov exponent, yet the geometric properties of the strange nonchaotic attractor is very similar to that of the chaotic attractor near the transition. Intuition would therefore suggest that the transition from the former to the latter results from only a nonabrupt change in the dynamical properties of the attractor. These dynamical properties could be, for instance, the expansion and contraction that a trajectory experiences in different phase-space regions. The geometric structure of the attractor should undergo almost no change when the transition occurs. Based on this intuition and numerical experiments, we propose the following scenario for the transition from strange nonchaotic to strange chaotic attractors. The phase-space region in which an attractor lives for chaotic dynamical systems, in general, can be divided into two subregions where a trajectory experiences either pure expansion or pure contraction. In particular, the expanding or the contracting region is the region where an infinitesimal vector in the tangent space either expands or contracts under the dynamics. One may then define the frequencies of visits to both the expanding and contracting regions. The Lyapunov exponent of the attractor is determined by the *average* expanding and contracting rates associated with both regions, respectively. Strange nonchaotic attractors occur when the average contracting rate weighs over the average expanding rate, rendering negative the asymptotic Lyapunov exponent. If, on the other hand, the average expanding rate weighs over the average contracting rate so that the Lyapunov exponent is positive, the attractor becomes strange chaotic. As a consequence of this picture, the Lyapunov exponent passes through zero linearly from the negative side as the transition occurs. We present numerical results verifying our transition scenario for (i) the quasiperiodically driven circle map and (ii) a more realistic physical system: the quasiperiodically forced pendulum, which includes as a special case the dynamics of a quantum particle in a quasiperiodical potential [2,3].

The organization of the paper is as follows. In Sec. II we describe the transition scenario in a more systematic way. In Sec. III we present numerical results with the quasiperiodically driven circle map. In Sec. IV we present results with the system of quasiperiodically forced pendulum. Discussions are presented in Sec. V.

II. THE TRANSITION SCENARIO

We consider quasiperiodically driven systems described by both discrete maps and flows, which are written as follows, respectively:

$$\mathbf{x}_{n+1} = \mathbf{F}(\mathbf{x}_n, p, \omega_1, \omega_2) \tag{1}$$

and

$$\frac{d\mathbf{x}}{dt} = \mathbf{F}(\mathbf{x}, p, \omega_1 t, \omega_2 t) , \tag{2}$$

where $\mathbf{x} \in \mathbf{R}^N$ (N is the phase-space dimension), $\mathbf{F}$ is the N-dimensional system evolution function, p is a system control parameter, and ω_1 and ω_2 are the two incom-

mensurate external driving frequencies. The transition from strange nonchaotic to strange chaotic attractors occurs at the critical parameter value $p = p_c$. Figure 1 schematically illustrates the division of the phase space into an expanding region I and a contracting region II for such a system. A trajectory resulting from a random initial condition visits both regions alternatively. Let $\Lambda_u(p)$ and $\Lambda_s(p)$ be the average expanding and contracting rate of the trajectory in the expanding and contracting regions, respectively. Let $f_u(p)$ and $f_s(p) = 1 - f_u(p)$ be the frequencies of visits of the trajectory to the expanding and contracting regions, respectively. In general, f_u and f_s also depends on the parameter p. The asymptotic Lyapunov exponent of the trajectory is thus given by

$$\Lambda(p) = f_u(p)\Lambda_u(p) - f_s(p)\Lambda_s(p) , \tag{3}$$

which also depends on the parameter p. Near the transition from a strange nonchaotic to a chaotic attractor, the geometric structures associated with both attractors are almost unchanged. Therefore, it is reasonable to assume that the phase-space structure shown in Fig. 1 is roughly the same for the strange nonchaotic and chaotic attractors for p in the vicinity of p_c. However, the dynamical properties of the attractors, as characterized by the quantities $\Lambda_u(p)$, $\Lambda_s(p)$, $f_u(p)$, and $f_s(p)$, change as the parameter p varies through the critical value p_c. Since the phase-space regions in which these quantities are defined do not change drastically, these quantities should have a smooth dependence on the parameter p. Expanding $\Lambda_u(p)$, $\Lambda_s(p)$, $f_u(p)$, and $f_s(p)$ around p_c using Taylor series and keeping only the first-order terms in $(p - p_c)$, we obtain

$$\Lambda(p) \approx A(p_c)(p - p_c) + B(p_c) , \tag{4}$$

where $A(p_c)$ and $B(p_c)$ are two constants that depend only on the critical parameter value p_c through the quantities $\Lambda_u(p_c)$, $\Lambda_s(p_c)$, $f_u(p_c)$, and $f_s(p_c)$ and their first derivatives evaluated at p_c. From Eq. (4), we see immediately that $\Lambda(p)$ passes through zero *approximately linearly* as the parameter p varies through p_c. This linear dependence is therefore a unique signature characterizing the transition from strange nonchaotic to strange chaotic attractors.
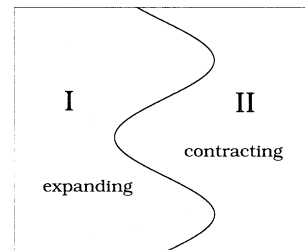

FIG. 1. Schematic illustration of the division of the phase space into expanding and contracting regions for quasiperiodically driven dynamical systems.

III. THE QUASIPERIODICALLY DRIVEN CIRCLE MAP

The quasiperiodically driven circle map is written as [4]

$$\phi_{n+1} = [\phi_n + 2\pi K + V \sin\phi_n + C \cos\theta_n]\mathrm{mod}(2\pi) ,$$
$$\theta_{n+1} = [\theta_n + 2\pi\omega]\mathrm{mod}(2\pi) ,$$
(5)

where both ϕ and θ are restricted in $[0, 2\pi]$ via the $\mathrm{mod}(2\pi)$ operation; K, V, and C are three parameters; and ω is irrational. It was shown in Ref. [4] that for Eq. (5) there are parameter regions of finite area where strange nonchaotic attractors exist. Furthermore, there exists a critical line in the two-dimensional parameter plane of K and V below and above which strange nonchaotic and chaotic attractors exist, respectively. Across this critical line, the transition from strange nonchaotic to chaotic behaviors occurs.

There are two Lyapunov exponents associated with Eq. (5). The one that corresponds to the θ dynamics is always zero. The other nontrivial exponent is given by

$$\Lambda = \lim_{n \to \infty} \frac{1}{n} \sum_{j=1}^{n} \ln|1 + V \cos\phi_j| .$$
(6)

Note that the Lyapunov exponent depends on all three parameters K, V, and C through the trajectory $\{\phi_j\}_{j=1}^{\infty}$. Choosing $K = 0.28$ and $C = 0.6$ in the parameter region investigated in Ref. [4], we find that the transition from strange nonchaotic to strange chaotic attractors occurs at $V = V_c \approx 1.07628$, where $\Lambda < 0$ for $V < V_c$ and $\Lambda > 0$ for $V > V_c$. For our subsequent numerical experiments, we shall concentrate on the parameter interval in the vicinity of V_c defined by $V \in [1.075, 1.078]$. Examination of the power spectra [4] of trajectories indicates that the attractors are strange for most values of V in $V < V_c$. Figure 2(a) shows a single trajectory resulting from an arbitrary initial condition on the strange nonchaotic attractor at $V = 1.075$. The Lyapunov exponent, computed by using 2×10^7 iterations, is $\Lambda \approx -0.01455$. The finite-time Lyapunov exponent Λ_n is shown in Fig. 2(b) for 2×10^4 iterations. It can be seen that Λ_n converges to the asymptotic value of approximately -0.01455 as $n \to \infty$. As a comparison, Fig. 3(a) shows a single trajectory on the chaotic side for $V = 1.078$. The Lyapunov exponent for this parameter value is estimated to be $\Lambda \approx 0.01193$. The finite-time exponent for this case is shown in Fig. 3(b). Evidently, without computing the Lyapunov exponents, it is visually difficult to distinguish the strange nonchaotic attractor in Fig. 2(a) from the strange chaotic attractor in Fig. 3(a). This suggests a rather smooth transition from the former behavior to the latter behavior.

To examine the phase-space structure on both sides of the transition, we first observe that the expanding and contracting regions are defined by $(|1 + V \cos\phi| > 1$, $\theta \in [0, 2\pi])$ and $(|1 + V \cos\phi| < 1$, $\theta \in [0, 2\pi])$, respectively. The two regions are thus given by $\theta \in [0, 2\pi]$ $(0 \le \phi < \pi/2$, $3\pi/2 \le \phi < 2\pi)$ (expanding) and $(\pi/2 \le \phi < 3\pi/2)$ (contracting) for $V > 0$. These two regions are invariant throughout the transition. Figures

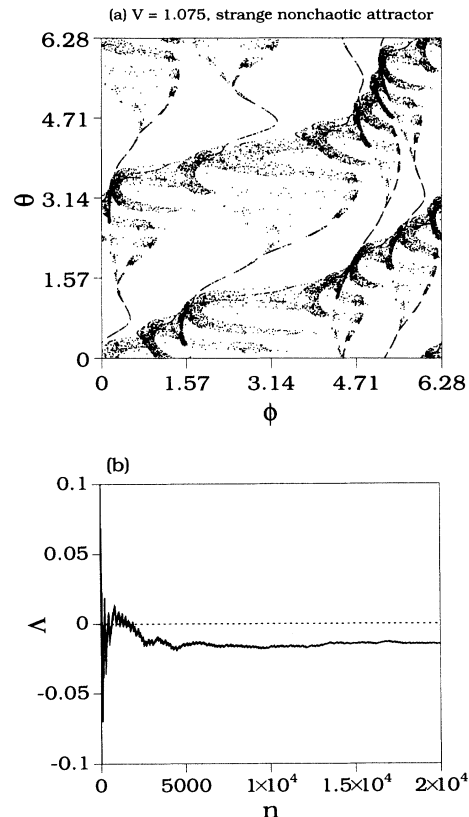(a) V = 1.075, strange nonchaotic attractor

(b)

FIG. 2. (a) Single trajectory on the strange nonchaotic attractor at $V = 1.075$ for the quasiperiodically driven circle map Eq. (5). Other parameter values are $K = 0.28$ and $C = 0.6$. (b) Finite time Lyapunov exponent computed for 2×10^4 iterations.

4(a) and 4(b) show, for $V = 1.075$, part of the trajectory of Fig. 2(a) in the expanding and contracting regions, respectively. The instantaneous variation of an infinitesimal vector, given by the quantity $L_n \equiv \ln|1 + V \cos\phi_n|$, along a trajectory on the strange nonchaotic attractor is shown in Fig. 4(c), where $L_n > 0$ (< 0) corresponds to the situation where the trajectory is in the expanding (contracting) region. It is evident that the trajectory visits both regions experiencing expansion or contraction alternatively. Figures 5(a)–5(c) show plots similar to Figs. 4(a)–4(c) for the case of chaotic attractor at $V = 1.078$. Visually, it is difficult to distinguish Figs. 4(a)–4(c) from Figs. 5(a)–5(c), indicating that the geometric structures for the strange nonchaotic and chaotic attractors are roughly the same near the transition point.

In order to verify our main result Eq. (4), we compute the relevant quantities Λ_u, Λ_s, f_u, and f_s throughout the transition region. We choose 300 values of V in [1.075, 1.078]. For each value of V, a random initial condition is chosen to yield a trajectory of length $N = 2 \times 10^7$. The frequencies of the visit to the expanding and contracting regions f_u and f_s are approximated by $f_u = N_u / N$ and $f_s = N_s / N$, where N_u and N_s are the numbers of trajectory points with $(0 \le \phi < \pi/2$, $3\pi/2 \le \phi < 2\pi)$ and

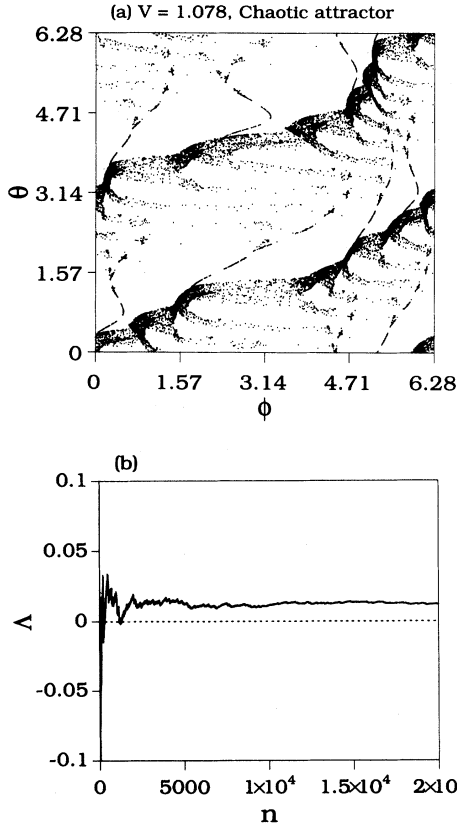(a) V = 1.078, Chaotic attractor

(b)

FIG. 3. (a) Single trajectory on the strange chaotic attractor at $V=1.078$. (b) Finite time Lyapunov exponent.

$(\pi/2 \leq \phi < 3\pi/2)$, respectively. The average expanding and contracting rates are then given by

$$\Lambda_u \approx \frac{1}{N_u} \sum_{j=1}^{N_u} \ln|1+V\cos\phi_j| , \tag{7}$$

$$\Lambda_s \approx \frac{1}{N_s} \sum_{j=1}^{N_s} \ln|1+V\cos\phi_j| .$$

Figures 6(a)–6(d) show Λ_u, f_u, Λ_s, and f_s versus the parameter V in the transition region. Clearly, all these four quantities behave approximately linearly as V passes through V_c, apart from numerical fluctuations due to finite length of the trajectory. Figure 7(a) shows the combinations $\Lambda_u f_u$ and $\Lambda_s f_s$ versus V. On the nonchaotic side of the transition, we have $\Lambda_u f_u < \Lambda_s f_s$. On the chaotic side, we have $\Lambda_u f_u > \Lambda_s f_s$. The transition occurs when $\Lambda_u f_u = \Lambda_s f_s$. Since $\Lambda_u f_u$ and $\Lambda_s f_s$ vary approximately linearly through the transition, the Lyapunov exponent Λ passes through zero also approximately linearly near the transition point, as shown in Fig. 7(b). This confirms our prediction Eq. (4).

IV. THE SYSTEM OF A QUASIPERIODICALLY FORCED PENDULUM

We now consider the quasiperiodically forced damped pendulum [3]

$$\frac{d^2\phi}{dt^2} + v\frac{d\phi}{dt} + \sin\phi = K + V[\cos(\omega_1 t) + \cos(\omega_2 t)] , \tag{8}$$

where ϕ is the angle the pendulum makes with the vertical axis, v is the dissipation rate, K is a constant, V is the forcing amplitude, ω_1 and ω_2 are the two incommensurate frequencies. Introducing the variable transform $t \rightarrow vt$ and $\phi \rightarrow \phi + \pi/2$, we rewrite Eq. (8) as

$$\frac{1}{p}\frac{d^2\phi}{dt^2} + \frac{d\phi}{dt} - \cos\phi = K + V[\cos(\omega_1 t) + \cos(\omega_2 t)] , \tag{9}$$

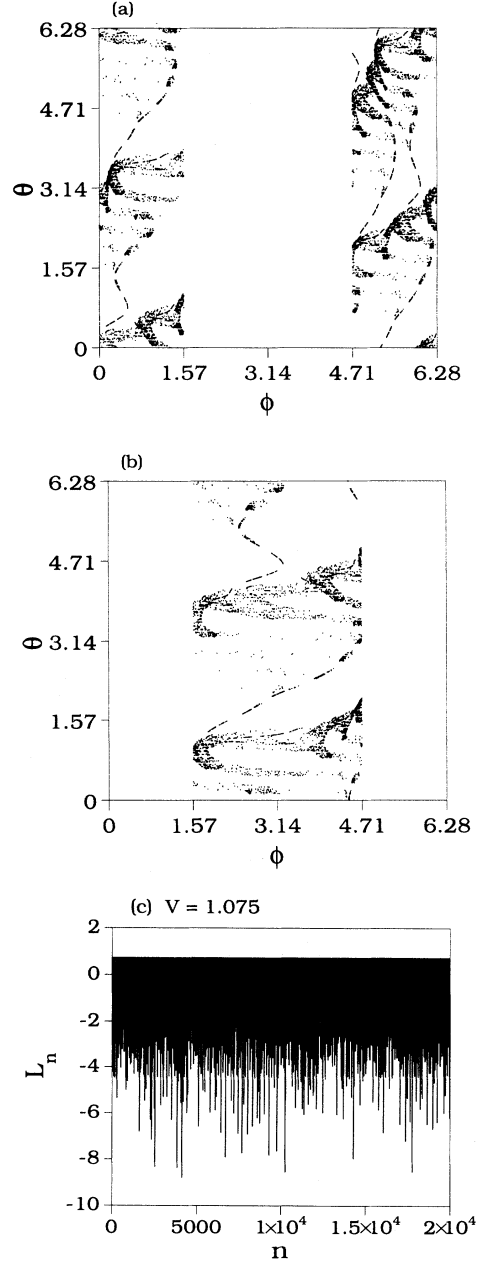
(a)

(b)

(c) V = 1.075

FIG. 4. Part of a long trajectory in (a) the expanding region and (b) the contracting region of the phase space for $V=1.075$. (c) Instantaneous variation of an infinitesimal tangent vector along the trajectory.

where $p = v^2$ is a new parameter and ω_1 and ω_2 have been rescaled accordingly: $\omega_1 \to \omega_1 v^{-1}$ and $\omega_2 \to \omega_2 v^{-1}$. In the strong damping limit $p \to \infty$, Eq. (9) reduces to a first-order equation that is isomorphic to the Schrödinger equation, which describes the dynamics of quantum particles in a quasiperiodic potential [2]. In terms of the dynamical variables ϕ, $v \equiv d\phi/dt$, and $z \equiv \omega_2 t$, Eq. (9) becomes
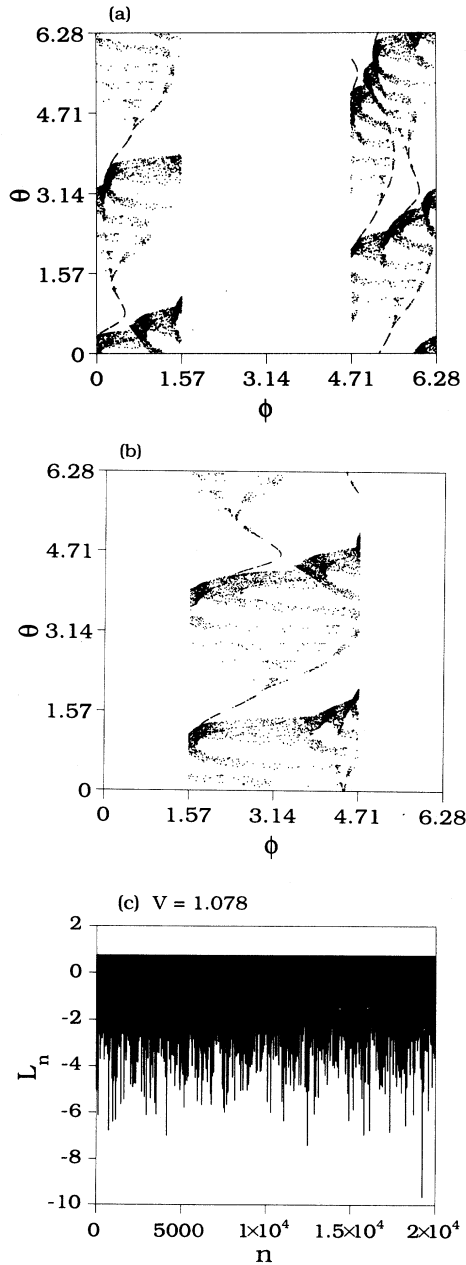

FIG. 5. Part of a long trajectory in (a) the expanding region and (b) the contracting region of the phase space for $V = 1.078$. A comparison with Figs. 4(a) and 4(b) indicates that the expanding and contracting regions for $V = 1.075$ (strange nonchaotic) and $V = 1.078$ (chaotic) are identical. (c) Instantaneous variation of an infinitesimal tangent vector along the trajectory.
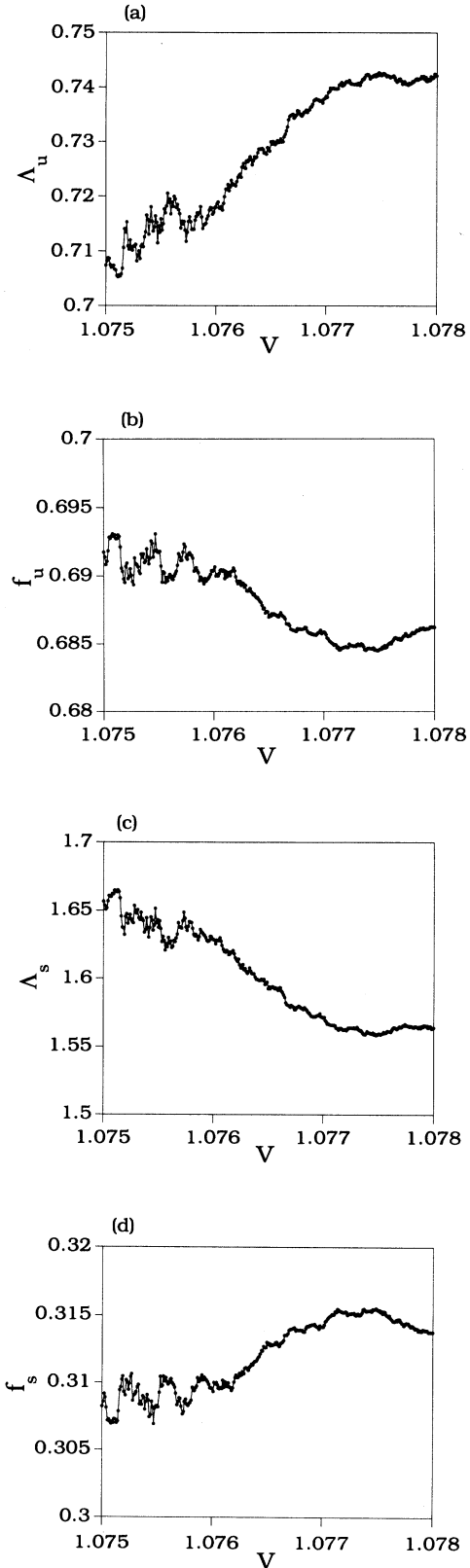

FIG. 6. Quantities (a) Λ_u, (b) f_u, (c) Λ_s, and (d) f_s versus the parameter V for $V \in [1.075, 1.078]$. Apart from numerical fluctuations due to the finite length of the trajectory, these quantities vary rather smoothly in the transition region.
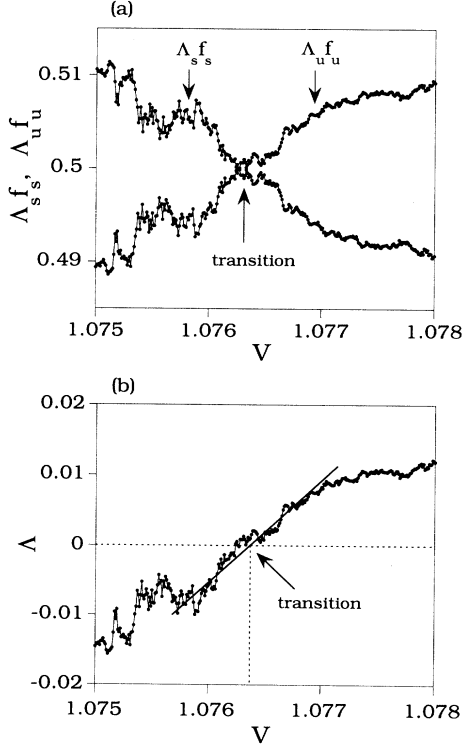
FIG. 7. (a) Combinations $\Lambda_u f_u$ and $\Lambda_s f_s$ versus the parameter V in the transition region. The transition from strange nonchaotic to strange chaotic attractors occurs when $\Lambda_u f_u = \Lambda_s f_s$. (b) Lyapunov exponent Λ versus the parameter V in the transition region. The exponent passes through zero approximately linearly at the transition.

$$\frac{d\phi}{dt} = v \ ,$$

$$\frac{dv}{dt} = p\left\{ K + V\left[\cos\left[\frac{\omega_1}{\omega_2}z\right] + \cos z\right] + \cos\phi - v\right\} \ ,$$

$$\frac{dz}{dt} = \omega_2 \ . \tag{10}$$

It has been shown that Eq. (10) exhibits rich dynamical phenomena [3]. In particular, there are parameter regions of finite areas where two- and three-frequency quasiperiodic attractors, strange nonchaotic attractors, and chaotic attractors exist.

For subsequent numerical experiments, we fix $K=0.8$, $V=0.55$, $\omega_1=(\sqrt{5}-1)/2$ (the golden mean), $\omega_2=1.0$, and choose p as the control parameter. For large values of p $(p>1.0)$, the damping is strong so that orbits are attracted to the torus rapidly and the torus is thus difficult to destroy. As p decreases, the contraction to the torus reduces and the torus can be destroyed [11]. For $p<p_0\approx1.0$, both strange nonchaotic and chaotic attractors exist. In fact, there are several parameter subintervals for $p\in[0,1]$ in which the transition from strange nonchaotic to chaotic attractors occurs. One such transition occurs at $p=p_c\approx0.6869$, where $\Lambda>0$ for $p\gtrsim p_c$ and
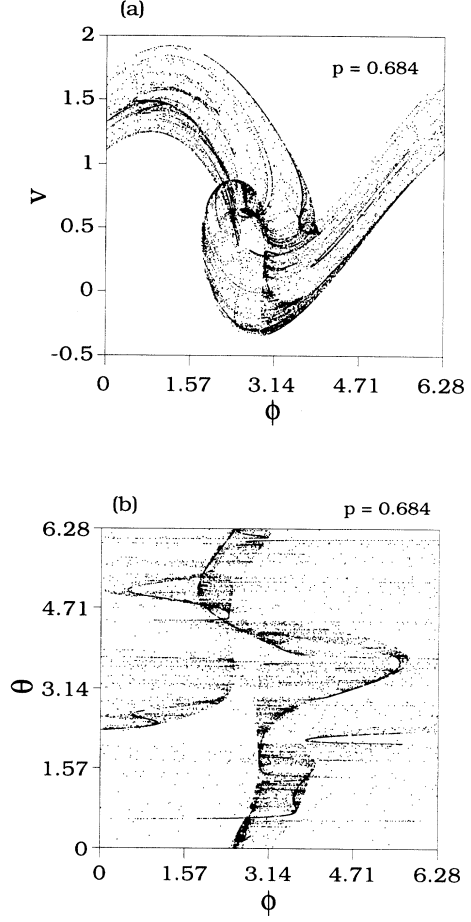

FIG. 8. (a) Stroboscopic attractor in the ϕ-v plane and (b) the attractor in the ϕ-θ plane for the quasiperiodically forced pendulum system Eq. (10) at $p=0.684$ (strange nonchaotic attractor). Other parameter values in Eq. (10) are $K=0.8$, $V=0.55$, ω_1 the golden mean, and $\omega_2=1$.

$\Lambda<0$ for $p\lesssim p_c$. The attractors for $p\gtrsim p_c$ are therefore chaotic. Here we shall concentrate on the small parameter interval $p\in[0.684,0.689]$ in the vicinity of p_c.

To visualize the attractors, it is convenient to use the Poincaré surface of section technique. Specifically, we sample the system at time intervals corresponding to the variable $z_n=\omega_2 t_n=2\pi n$, where $n=0,1,\ldots$ (the stroboscopic surface of section). We then examine the dynamical variables $\phi_n(\text{mod}2\pi)$, v_n, and $\theta_n\equiv\omega_1 t_n(\text{mod}2\pi)$ on the surface of section. Examination of the attractors for $p\lesssim p_c$ indicates that they are nonchaotic, yet they are geometrically strange, as shown in Figs. 8(a) (the ϕ_n versus v_n plot) and 8(b) (the ϕ_n versus θ_n plot) for $p=0.684$ ($\Lambda\approx-0.0096$). As a comparison, Figs. 9(a) and 9(b) show a single long trajectory on the chaotic attractor for $p=0.689$ ($\Lambda\approx0.0079$), where ϕ_n versus v_n and ϕ_n versus θ_n are plotted in (a) and (b), respectively.

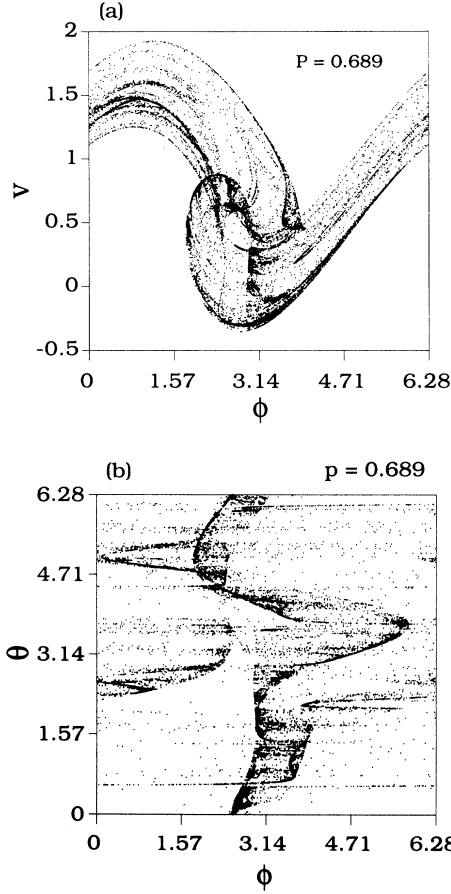To compute the Lyapunov exponents, we take the variations of the dynamical variables in Eq. (10) to obtain

(a)

P = 0.689

(b)   p = 0.689

FIG. 9. (a) Stroboscopic attractor in the ϕ-v plane and (b) the attractor in the ϕ-θ plane for the quasiperiodically forced pendulum system Eq. (10) at $p = 0.689$ (strange chaotic attractor).

(a)   p = 0.684, expanding region

(b)   p = 0.684, contracting region

FIG. 10. (a) Expanding and (b) contracting regions for $p = 0.684$.

$$\frac{d\delta\phi}{dt} = \delta v \ ,$$

$$\frac{d\delta v}{dt} = -p\left\{\left[(V\omega_1/\omega_2)\sin\left[\frac{\omega_1}{\omega_2}z\right] + \sin z\right]\delta z \right.$$

$$\left. + \sin\phi\,\delta\phi + \delta v\right\} \ ,$$ (11)

$$\frac{d\delta z}{dt} = 0 \ .$$

Note that the dynamics in z and δz gives rise to a Lyapunov exponent that is always zero. The maximum nontrivial Lyapunov exponent is given by

$$\Lambda = \lim_{t\to\infty} \frac{1}{t}\ln\frac{\Delta(t)}{\Delta(0)} \ ,$$ (12)

where $\Delta(t) \equiv \sqrt{\delta\phi^2(t) + \delta v^2(t)}$. The quantities Λ_u, Λ_s, f_u, and f_s in Eq. (3) can be evaluated by monitoring successive passes of a long trajectory through the surface of section. Specifically, we compute values of the quantity $\ln[\Delta(t)/\Delta(0)]$ averaged over the time interval $T \equiv 2\pi/\omega_2$. If the average value $(1/T)\int_0^T\ln[\Delta(t)/\Delta(0)]dt > 0$ (< 0), then it is taken to be
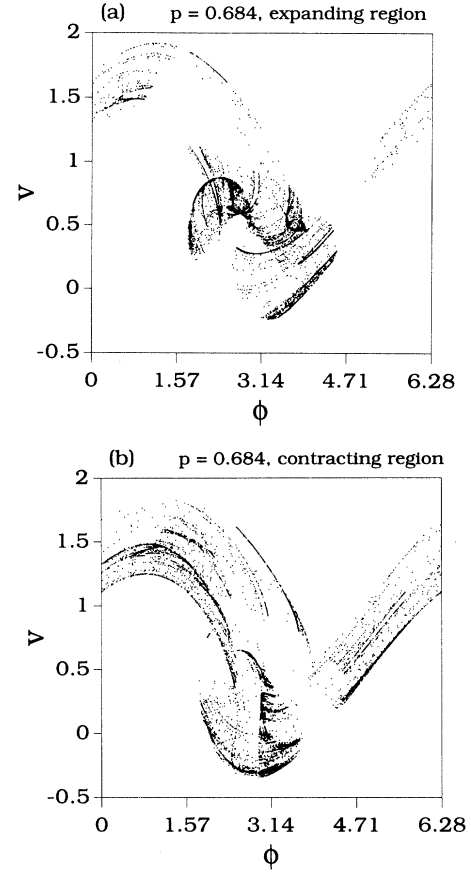
Λ_u (Λ_s) for one iteration on the surface of section. The quantities f_u and f_s are the frequencies of having Λ_u and Λ_s, respectively, for a long trajectory. Figures 10(a) and 10(b) show part of the trajectory with $(1/T)\int_0^T\ln[\Delta(t)/\Delta(0)]dt > 0$ and $(1/T)\int_0^T\ln[\Delta(t)/\Delta(0)]dt < 0$, respectively, on the surface of section for $p = 0.684$ (strange nonchaotic attractor). The corresponding plots for $p = 0.689$ (chaotic attractor) are shown in Figs. 11(a) and 11(b). Evidently, the expanding and contracting regions on the surface of section remain approximately the same as p varies from 0.684 to 0.689, indicating that the geometric structures for the strange nonchaotic and chaotic attractors near the transition does not change appreciably. The quantities Λ_u, f_u, Λ_s, and f_s, however, change slowly as p is increased passing through the critical value p_c. Figure 12(a) shows the combinations of $\Lambda_u f_u$ and $\Lambda_s f_s$ versus the parameter p for $p \in [0.684, 0.689]$ and Fig. 12(b) shows the Lyapunov exponent Λ versus p. Clearly, near the transition point, the Lyapunov exponent Λ passes through zero approximately linearly. The small amplitude fluctuations on the curves in Figs. 12(a) and 12(b) are the artifacts of the numerical computation in which the integration time and the transient time are $40\,000(2\pi/\omega_2)$ and $2000(2\pi/\omega_2)$, respectively, for each of the 500 values of p in Figs. 12(a)
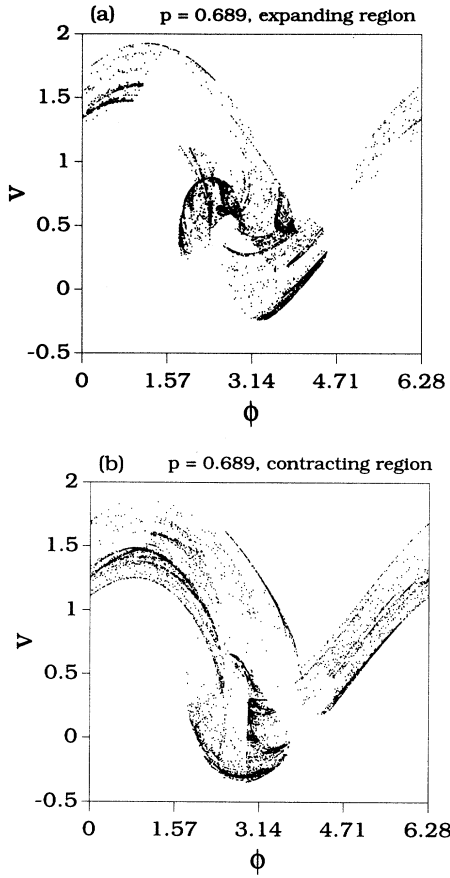
FIG. 11. (a) Expanding and (b) contracting regions for $p=0.689$.

FIG. 12. (a) Combinations $\Lambda_u f_u$ and $\Lambda_s f_s$ versus the parameter p in the parameter region $p \in [0.684, 0.689]$ in the vicinity of the transition. (b) Lyapunov exponent Λ versus the parameter p in the transition region. The exponent passes through zero approximately linearly at the transition.

and 12(b). Choosing longer integration and transient times can reduce the numerical fluctuations, which is, however, computationally intense. In spite of the numerical fluctuations, the transition from strange nonchaotic to chaotic attractors here is similar to that in the quasi-periodically driven map Eq. (5). This is actually expected because, on the surface of section, the dynamics of the flow generated by Eq. (10) is equivalent to that of a map driven quasiperiodically.

V. DISCUSSION

The main conclusion of the paper is that in quasi-periodically driven dynamical systems, the transition from strange nonchaotic to strange chaotic attractors follows the route in which the Lyapunov exponent passes through zero linearly from the negative side to the positive side. This can be understood by studying the structure of the phase space in which the strange nonchaotic and chaotic attractors lie for parameter values near the transition. We have developed an approach to examine the phase space that is particularly suitable for investigating this type of transition. Specifically, we divide the phase space into regions where infinitesimal tangent vectors along a trajectory experience expansion or contrac-
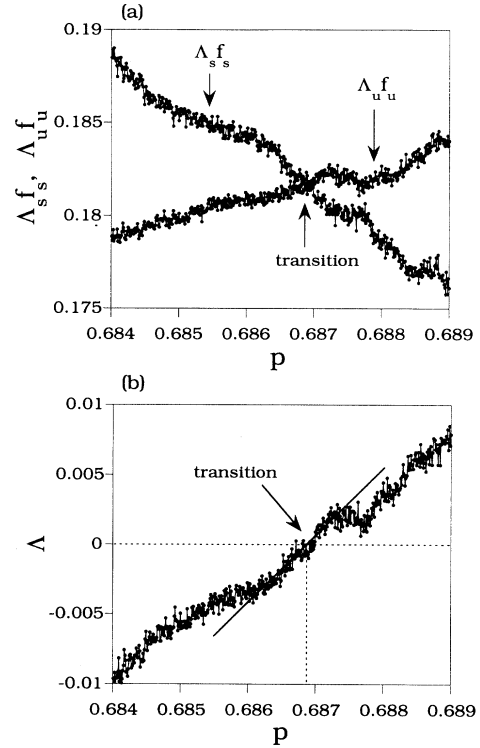
tion. We then compute the frequencies of the visit to both regions and also the average expanding and contracting rates in both regions. These quantities change smoothly as the parameter changes through the critical value at which the transition occurs. Whether the asymptotic attractor of the system is strange nonchaotic or strange chaotic is determined by the relative weights of the expanding and contracting rates. The attractor is strange nonchaotic if the contracting rate weighs over the expanding rate. Otherwise the attractor is strange chaotic. This scenario for the transition from strange nonchaotic to chaotic attractors was verified using both a quasiperiodically driven map and a quasiperiodically driven flow. We conjecture that this route to chaotic attractors is a general route to chaos in quasiperiodically driven dynamical systems.

It is interesting to review the possible routes to chaotic attractors in nonlinear dynamical systems in general. So far there are four known major routes to chaotic attractors: (i) the period-doubling cascade route [8], (ii) the intermittency transition route [12], (iii) the Ruelle-Takens route for quasiperiodic flows [13], and (iv) the crisis route [14]. In route (i), a chaotic attractor appears in a parameter region immediately following the accumulation of an infinite number of period doublings. Feigenbaum showed that there are universal quantitative behaviors for the

period-doubling cascade [8]. Near the transition point, the largest Lyapunov exponent exhibits nondifferentiable variations as it passes through zero from the negative side. In route (ii), as a parameter passes through a critical value, a simple periodic orbit is replaced by a chaotic attractor in such a way that the chaotic behavior is interspersed with a periodic behavior resembling that before the transition in an intermittent fashion. The average duration of the chaotic bursts scales algebraically with the parameter variation above the critical value [12]. In route (iii), a quasiperiodic flow is substituted by a strange attractor on the torus. In the parameter space, the quasiperiodic flow occurs at a Cantor set of parameter values, while the strange attractor occurs at the complement of the Cantor set. In route (iv), a chaotic attractor is suddenly created to replace a nonattracting chaotic saddle as the parameter passes through the crisis value [14]. In this case, the Lyapunov exponent for the attractor is defined only after the chaotic attractor is born. All four routes to chaotic attractors have been observed in many physical systems [15]. The route to chaos discussed in this paper [16] for quasiperiodically driven systems appears to be fundamentally different from these four known routes to chaos.

[1] C. Gebrogi, E. Ott, S. Pelikan, and J. A. Yorke, Physica D **13**, 261 (1984).

[2] A. Bondeson, E. Ott, and T. M. Antonsen, Jr., Phys. Rev. Lett. **55**, 2103 (1985).

[3] F. J. Romeiras and E. Ott, Phys. Rev. A **35**, 4404 (1987); F. J. Romeiras, A. Bondeson, E. Ott, T. M. Antonsen, Jr., and C. Grebogi, Physica D **26**, 277 (1987).

[4] M. Ding, C. Grebogi, and E. Ott, Phys. Rev. A **39**, 2593 (1989).

[5] J. F. Heagy and S. M. Hammel, Physica D **70**, 140 (1994).

[6] A. S. Pikovsky and U. Feudel, Chaos **5**, 253 (1995).

[7] A. S. Pikovsky and U. Feudel, J. Phys. A **27**, 5209 (1994); U. Feudel, J. Kurths, and A. S. Pikovsky, Physica D (to be published).

[8] M. J. Feigenbaum, J. Stat. Phys. **19**, 25 (1978).

[9] W. L. Ditto, M. L. Spano, H. T. Savage, S. N. Rauseo, J. F. Heagy, and E. Ott, Phys. Rev. Lett. **65**, 533 (1990).

[10] S. P. Kuznetsov, A. S. Pikovsky, and U. Feudel, Phys. Rev. E **51**, R1629 (1995).

[11] The quasiperiodically forced pendulum has two nontrivial Lyapunov exponents Λ and Λ' that satisfy $\Lambda' = -(p + \Lambda)$, where p is the damping rate in Eq. (10). This can be seen by noting that Eq. (10) is actually a time-dependent flow of the form $d\phi/dt = v$ and $dv/dt = -p(v - \cos\phi) + f(t)$. Taking the divergence of this flow, we obtain $(\partial/\partial v)(dv/dt) + (\partial/\partial\phi)(d\phi/dt) = -p$. Since this divergence is also the sum of the Lyapunov exponents, Eq. (13) holds. For large values of p, both Λ and Λ' are negative. The exponent Λ' can be viewed as the exponential rate at which orbits in the three-dimensional phase space (ϕ, v, z) are attracted to the torus. For large p the rate is large, rendering the torus stable and difficult to destroy. As p decreases, $-\Lambda'$ becomes smaller. For $p \lesssim 1$ the nonlinearity can destroy the torus since the contraction to the torus is weak [3].

[12] Y. Pomeau and P. Manneville, Commun. Math. Phys. **74**, 189 (1980).

[13] D. Ruelle and F. Takens, Commun. Math. Phys. **20**, 167 (1971); S. Newhouse, D. Ruelle, and F. Takens, ibid. **64**, 35 (1978).

[14] C. Grebogi, E. Ott, and J. A. Yorke, Phys. Rev. Lett. **48**, 1507 (1982); Physica D **7**, 181 (1983).

[15] For example, J. Gollub and H. L. Swinney, Phys. Rev. Lett. **35**, 927 (1975); A. Libchaber and J. Maurer, J. Phys. (Paris) Colloq. **41**, C3 (1980); J. P. Gollub and S. V. Benson, J. Fluid Mech. **100**, 449 (1980); P. Linsay, Phys. Rev. Lett. **47**, 1349 (1981); J. C. Sommerer, W. L. Ditto, C. Grebogi, E. Ott, and M. L. Spano, Phys. Lett. A **153**, 105 (1991).

[16] Transition to chaos characterized by a linearly passing through zero of the Lyapunov exponent has also been identified in random maps. See L. Yu, E. Ott, and Q. Chen, Phys. Rev. Lett. **65**, 2935 (1990); Physica D **53**, 102 (1991).